Vol. 48 No. 1 Journal of the Communications Research Laboratory March 2001
Printed in Tokyo, Japan pp. 73–81

3.2 Development of Dicke-type Radiometer for 22 GHz Band

By
Hiroshi OKUBO, Yasuhiro KOYAMA, Mamoru SEKIDO, and Eiji KAWAI

ABSTRACT

For radio astronomy observations, the 22-GHz band is important as an observation frequency band for H_2O maser-line spectrum emission from active regions in galaxies. For continuum-emission observations, however, 22 GHz has some disadvantages. In general, non-thermal emission becomes weaker at high-microwave frequency bands, and water-vapor atmospheric absorption and emission degrades signals from the radio source and increases antenna noise. Consequently, 22-GHz continuum-emission observations are more difficult than observations at lower frequencies. In response to this problem, we have been developing a Dicke-type switching radiometer for single dish observation of continuum-emission sources. In this paper, we report on the configuration of this system and results of experimental observations using a reference radio source.

Keywords: Total power observation, Dicke switching

1. Introduction

The 22-GHz band plays an important role in radio astronomy observations as the frequency band of water-maser radio sources. In continuum-emission observations, however, the 22-GHz band suffers from several problems. For example, the intensity of continuum-emission sources due to non-thermal emission becomes weaker as the observation frequency becomes higher, and intensity fluctuation caused by atmospheric absorption and emission can be severe. In addition, lowering receiver noise is more difficult at high frequencies than at low frequencies. Data must therefore be processed carefully when measuring beam pattern, aperture efficiency, and other characteristics by observing continuum-emission source intensity with a single dish.

Against the above background, we have been developing a beam switch based on classical Dicke-type switching with the goal of detecting continuum-emission source with high signal-to-noise ratio observations.

When using beam switching observe radio source, the system alternates between the antenna's main beam pointing at the radio source and a reference beam pointing at another point in the sky. Then, by subtracting the power of the reference beam from that of the main beam, slight additional noise originating in the radio source can be detected[(1)(2)]. The speed of this switching is made to be faster than the speed of both atmospheric fluctuation, the cause of fluctuation in antenna output, and fluctuation in system gain. As a result, the effects of these fluctuations can be removed and the intensity of radio waves arriving from radio sources can be correctly measured.

In this article, we first provide an overview of observation equipment. We then report on a test observation using a radio source whose flux is known, and discuss system evaluation and antenna calibration based on the results of those observations.

2. Basic Concepts

2.1 Antenna output and antenna temperature

Given that the main beam is pointing at a radio source, the observed quantities for one operation cycle of an ideal beam switch are main-beam output P_{On} and reference-beam output P_{Off}, which can be expressed as follows.

$$P_{On} = k[T_{LNA} + T_{Atm}(t)(1-\exp(-\tau \sec Z)) + T_A \exp(-\tau \sec Z)]G(t)B$$

$$P_{Off}^{Sw} = k[T_{LNA} + T_{Atm}(t)(1-\exp(-\tau \sec Z))]G(t)B \quad \cdots\cdots (1)$$

Here:
k = Boltzmann constant
T_{LNA} = receiver noise temperature
T_{Atm} = physical temperature of atmosphere
T_A = antenna temperature: energy from radio source incident on antenna (value of energy from outside of atmosphere)
τ = optical thickness of atmosphere in zenith direction

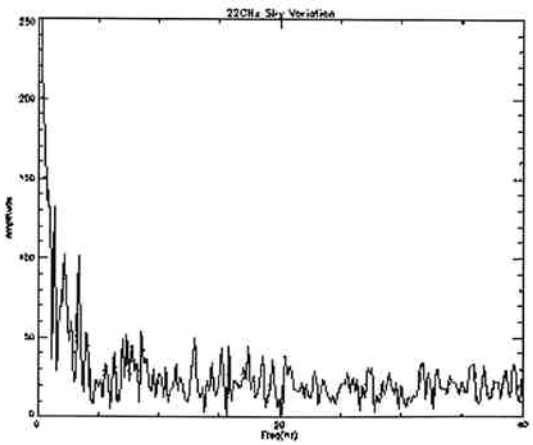

Fig. 1 Power spectrum of antenna output when observing the zenith

G = receiver gain
B = receive bandwidth
Z = zenith angle

Figure 1 shows the frequency spectrum of fluctuating components obtained by performing a fast Fourier transform on antenna output when observing the sky for five seconds with the antenna pointed toward the zenith. As shown, significant fluctuation exists under 5 Hz. It is considered, however, that such effects can be removed by beam switching.

Antenna-incident atmospheric radiation and receiver gain are treated as time functions. In this regard, beam switching observes the main beam and reference beam in a period that is shorter than atmospheric fluctuation, and takes the difference between the values of main and reference beams to remove fluctuating components from atmospheric radiation $T_{Atm}(1-\exp(-\tau\sec Z))$ and to extract the power added by the radio source. For the case that fluctuating components have been completely removed, the result of subtracting reference-beam output from main-beam output can be expressed as follows.

$$P_{On}-P_{Off}^{Sw} = kT_A \exp(-\tau \sec Z) GB \quad \cdots\cdots (2)$$

Here, the term $\exp(-\tau \sec Z)$ that is multiplied by antenna temperature T_A represents the amount of energy from the radio source that is absorbed by the atmosphere, τ is optical thickness of the atmosphere in the zenith direction, and Z is the zenith angle. In general, the value of τ can be determined to a certain level of accuracy by making chipping observations before and after the observation in question[3][4][5].

To determine the absolute value of GB in the above expression, we consider the following expression for antenna output when measuring a radio-wave absorber at room temperature within a short period in which gain G does not vary.

$$P_{Hot} = k[T_{LNA}+T_{Hot}]GB$$

Solving for GB, we get the following expression.

$$GB = \frac{P_{Hot}}{k[T_{LNA}+T_{Hot}]} \quad \cdots\cdots (3)$$

If T_{LNA} is known, the right side of the above equation is completely determined, and T_A, the basic observed quantity when observing a radio source by a single dish, can be computed as follows.

$$T_A \exp(-\tau \sec Z) = \frac{(P_{On}-P_{Ref})(T_{LNA}+T_{Hot})}{P_{Hot}}$$

$$T_A = \left(\frac{(P_{On}-P_{Ref})(T_{LNA}+T_{Hot})}{P_{Hot}}\right)\exp(\tau \sec Z) \quad \cdots\cdots (4)$$

2.2 Quantity expressing antenna temperature T_A

Observed quantity T_A determined by Eq. (4) can also be expressed by the following relationship if the radio source is considered to be sufficiently small with respect to antenna beam size[1][2].

$$kT_A = \frac{1}{2}A_e S_\nu \quad \cdots\cdots (5)$$

A_e : Effective aperture area
S_ν : Flux density

Here, flux density S_ν is radio-source intensity per unit time, unit area, and unit frequency when observing energy from a radio source from outside the atmosphere. The coefficient 1/2 takes into account that fact that only one component (one direction) of received polarization is treated.

From the above relationship, the antenna's effective aperture area A_e at a certain frequency and aperture efficiency η_A can be determined as follows.

$$A_e = \frac{2kT_A}{S_\nu} \quad \cdots\cdots (6)$$

$$\eta_A = \frac{A_e}{\frac{\pi}{4}D^2} \quad \cdots\cdots (7)$$

D: Antenna aperture

If the antenna's effective aperture area is known, unknown effective flux density S_ν incident on the antenna can be determined as follows.

$$S_\nu = \frac{2kT_A}{A_e} \quad \cdots\cdots (8)$$

3. Observation Equipment

3.1 Front-end equipment

In developing the front end for this observation equipment, space on the 22-GHz feed trolley had to be taken into account.

The Kashima 34-m antenna allows for multifrequency observations by an original band-interchange system. The drawback of this system, however, is that there is not much leeway in the space used for installing the receiver, which means that the space available for installing large components or observation equipment is limited. Consequently, installing large devices like a conventional chopper-type beam switch[2] is difficult. Under these circumstances, we decided to design and construct a compact front end.

Here, the reference beam is achieved by blocking the beam by a primary reflection panel tilted at an angle of 45° in front of a feed horn placed at the Cassegrain focus and then by reflecting the beam again by a secondary reflection panel tilted at an angle of 45°. In conventional chopper-type beam switches, the primary reflection panel rotates in the horizontal direction above the feed horn (the axis of rotation is parallel to the feed direction). This means that the primary and secondary reflection panels together take up much room, which is incompatible with the 34-m antenna. For this reason, we devised a system whereby the lower side of a rectangular-shaped primary reflection panel is made the axis of rotation and the panel is moved like a round fan above the feed horn (Figs. 2 and 3). Atmospheric effects due to elevation angle are taken into account by offsetting the reference

beam in the azimuth direction. In observations using the moon, the reference beam observes the sky at an offset of $-0.35°$ in the azimuth direction with respect to the main beam.

To simplify the equipment, we opted for a system that processes observation results at the software level instead of using closed-loop control in the drive motors. The number of operating rotations is about 180 rpm, and to achieve smooth rotation, balance weights are installed on the rotation axis.

While measuring the level of a radio-wave absorber at room temperature is essential to observation data, carrying out such measurements with such equipment in its original form is difficult within the limited space provided. We therefore substituted a waveguide switch for this equipment. Here, however, switching waveguides takes time, and the number of observation data items that can be used is consequently limited. The characteristics of the 22-GHz receiver of the 34-m antenna are listed in Table 1.

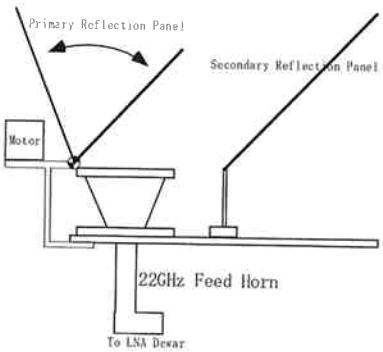

Fig. 2 Outline of 22-GHz beam switch

3.2 Signal transmission system

The signal transmission system is the same as an ordinary 22-GHz observation side. The configuration of the 22-GHz receiver system is shown in Fig. 4. In this system, the signals (at observation frequencies of 21.8-23.8 GHz) from the radio source incident on the 34-m antenna pass through the radome via the main reflector and subreflector and converge at the Cassegrain focus in the Feed Room. Then, through the use of a corrugated horn and waveguide, the signals are input into a low noise amplifier (LNA) cooled down to about 10K within the dewar and amplified. These receive signals amplified by the LNA are next converted to intermediate frequencies of 5-7 GHz by a down-converter on the same trolley, and finally transmitted by an optical transmitter to the Observation Room where they are again down converted to 0-2 GHz.

3.3 Data recording system

Observations using beam switching require that data be recorded at high time resolution. In addition, a large time constant as used in a power meter is not suitable. This is because receiver output when switching beams varies significantly over a short period of time since something other than the sky is being observed at this time. To resolve this problem, we chose to perform squared detection on the 0-2 GHz IF signals using a detector with a small time constant. Figure 5 shows that the time constant of the detector used here is less than 1 msec. Taking this detector time constant into account, signals are recorded at 48 kHz and are averaged at the first stage of data processing into 1-kHz sampled data.

Negative voltage output from the detector is reversed amplified at an operational amplifier and recorded in a

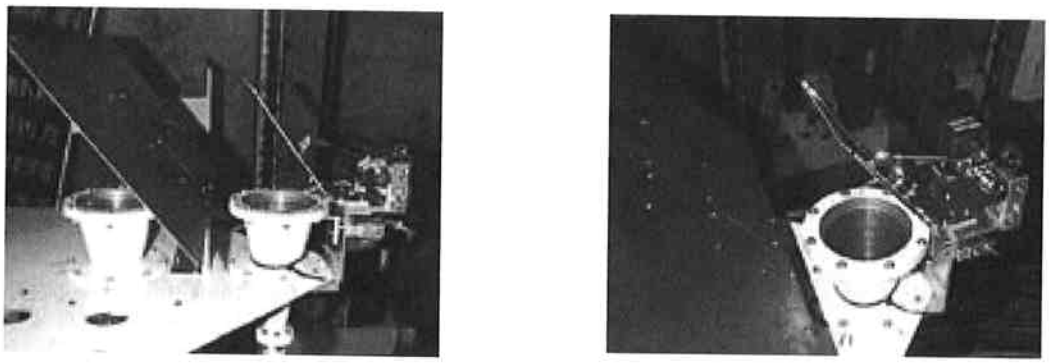

Fig. 3 Beam switch installed on 22-GHz feed trolley

Table 1 Main characteristics of 22-GHz receiver of Kashima 34-m antenna

LNA Type	Receive Polarization	Receive Frequency	Receiver Noise Temperature (TRX)	System Noise Temperature (Tsys)	SEFD (DR21)
Cooled HEMT	L/RHCP	21800MHz-23800MHz	280K	320K	2600Jy

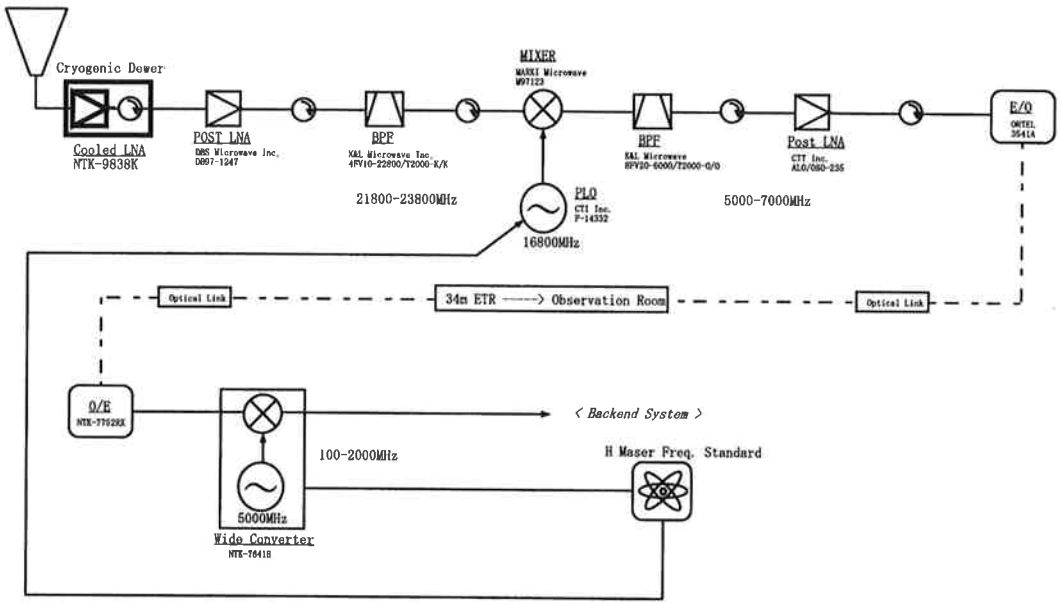

Fig. 4 System diagram of 22-GHz receiver of Kashima 34-m antenna

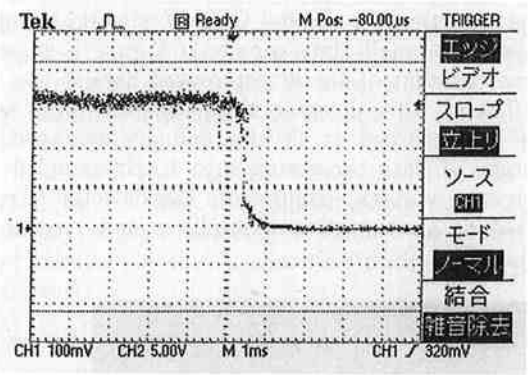

Fig. 5 Step response of detector; change in detector output when changing input level by step attenuator
X-axis: 1msec/Div. Y-axis: 100mV/Div.

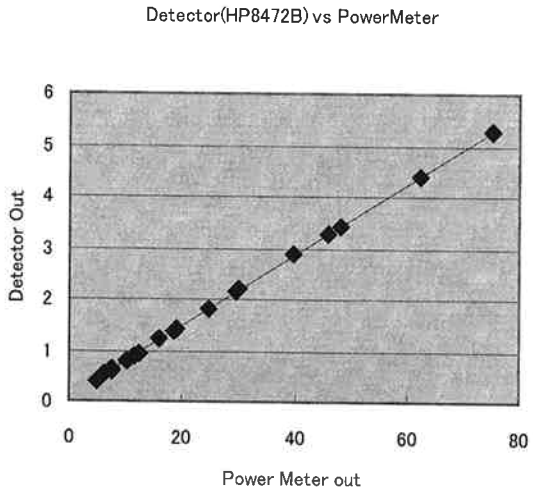

Fig. 6 Detector characteristics; X-axis: input level, Y-axis: detector output

range of ±1V on a Digital Audio Tape (DAT) recorder (48-KHz, 16-bit sampling). To decrease quantized noise at this time, level adjustments are performed in the attenuator and operational-amplifier circuits so as to raise maximum sensitivity in the ±1V range. Likewise, DC offset is not removed to prevent unnecessary causes of error. Input/output characteristics of the detector are shown in Fig. 6. Here, care was taken to use the linear section of the detector by limiting the input level. Characteristics of the reverse amplifier are shown in Fig. 7 and input/output characteristics of the entire system are shown in Fig. 8. As shown, we have been able to achieve linear characteristics in the system on up to the detector and DAT recorder.

The DAT recorder, however, automatically performs level adjustments before recording commences. For this reason, we record signals with differ input levels at the power meter and DAT recorder before an observation and determine the offset caused by the DAT recorder. This offset is then removed from obtained data and the result is treated as observation data.

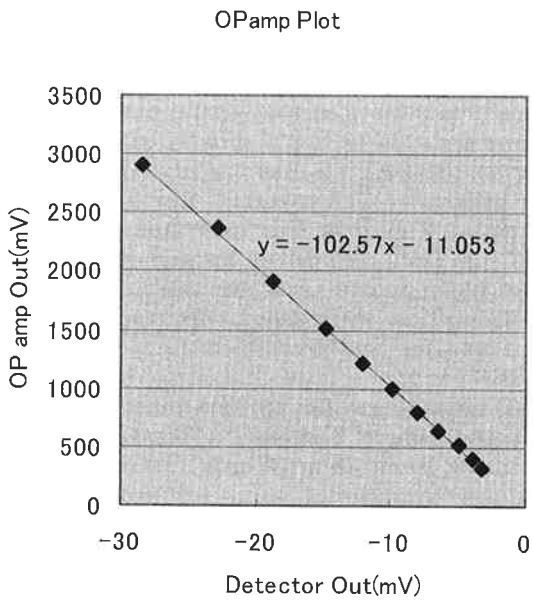

Fig. 7 Characteristics of reverse amplifier; X-axis: input level, Y-axis: amplifier output

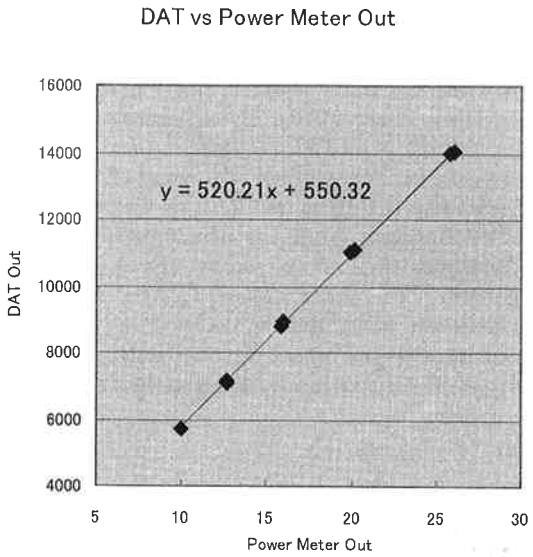

Fig. 8 DAT recorder output: X-axis: input level, Y-axis: DAT recorder output

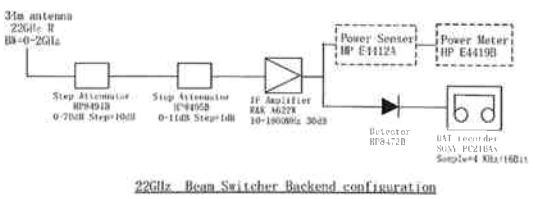

Fig. 9 System diagram of 22-GHz beam-switch back end; power meter is used for calibrating DAT recorder before observation

4. Observation

4.1 Characteristics of beam-switch output

Time-series data obtained when actually operating the beam switch and observing the sky with no radio source are shown in Fig. 10.

Specifically, this figure shows data for one second when observing the sky with a beam-switching period of about 0.22 second. The section of low output in one period is main-beam output while the two peaks of high output are the result of observing the inside wall of the feed cone when switching between beams and are therefore meaningless as data. In addition, the narrow region sandwiched between these two peaks corresponds to the time that the reference beam faces the sky with no radio source. This time makes up about 10% of observation time within one period. These time-series data are processed in units of 0.3 second at the data processing stage.

As shown in the figure, there is a difference between main-beam output P_{Off} and reference-beam output P_{Off}^{Sw} when viewing the sky with no radio source. This is attributed not to the fact that the reference beam faces the sky just as the main beam does, but rather to loss in the reference beam due to reflection off of two reflection panels and to viewing by part of the reference beam of the inner wall of the feed cone. If we now take this effect into account and represent it as loss factor α due to beam switching, we can rewrite Eq. (1) for the observed signal as follows[6]. We can also express antenna output P_{On} when pointing the main beam at a radio source and antenna output P_{Off} when viewing just the sky as shown below.

$$P_{Off}^{Sw}=k[T_{LNA}+T_{Atm}(1-\exp(-\tau\sec Z))(1-\alpha)+\alpha T_{Room}]GB$$

$$P_{On}=k[T_{LNA}+T_{Atm}(1-\exp(-\tau\sec Z))+T_{A}\exp(-\tau\sec Z)]GB$$

$$P_{Off}=k[T_{LNA}+T_{Atm}(1-\exp(-\tau\sec Z))]GB \quad \cdots\cdots (9)$$

T_{Room} : room temperature

The quantity ΔP^{Sw} denoting noise added to the reference beam by beam switching can be expressed as follows when both the main beam and reference beam are observ-

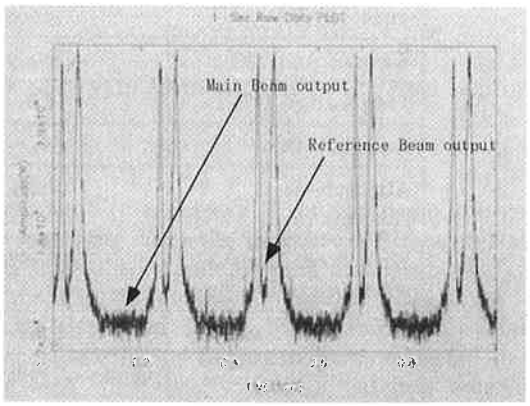

Fig. 10 Time-series data of beam-switch output; shows data over one second

ing the sky with no radio source and the assumption is made that $T_{Room} = T_{Atm}$.

$$\Delta P^{Sw} = P_{Off}^{Sw} - P_{Off} = k[\alpha T_{Atm}\exp(-\tau\sec Z)]GB \quad \cdots\cdots\cdots (10)$$

From this equation, loss factor α can be solved as follows.

$$\alpha = \frac{P_{Off} - P_{Off}^{Sw}}{kT_{Atm}\exp(-\tau\sec Z)GB} \quad \cdots\cdots\cdots (11)$$

Now, by determining loss factor α of the reference beam beforehand and measuring a radio-wave absorber at room temperature in a short time period in which gain fluctuation can be ignored, we can express radio-source intensity T_A as follows from Eqs. (3) and (4) by incorporating actual beam-switch characteristics.

$$T_A\exp(-\tau\sec Z) = \frac{(P_{On} - P_{Off}^{Sw})(T_{LNA} + T_{Hot})}{P_{Hot}} + \alpha T_{Atm}\exp(-\tau\sec Z)$$

$$T_A = \left(\frac{(P_{On} - P_{Off}^{Sw})(T_{LNA} + T_{Hot})}{P_{Hot}}\right)\exp(\tau\sec Z) + \alpha T_{Atm} \quad \cdots\cdots\cdots (12)$$

4.2 Test observation

Using this beam switch, we conducted a test observation on November 29, 2000. Meteorological data for this day is given in Table 2.

In this observation, we used a radio source with known flux density and calculated and evaluated observed quantity T_A from data obtained by beam switching using Eq. (12).

Since this was a test observation, another of our objectives was to measure attenuation (loss factor α) originating in the beam switch. To this end, the actual observation was performed by the following procedure.

Pointing the main beam at the radio source, the waveguide switch is switched about every 30 seconds to perform hot/cold observations. Next, the main beam is moved away from the radio source and hot/cold observations are performed again in the same way as above. Repeating this process gives us observation data, but one switching routine is treated as one session. Before actually activating the beam switch, moreover, a chipping observation was performed to measure optical thickness of the atmosphere. In addition, directly after initiating recording by the DAT recorder, input level was varied by a step attenuator and recorded simultaneously at the power meter. This data was used later to calculate the offset of the DAT recorder as mentioned above.

The radio source that we used here was DR21 (2037+421). This radio source features intensity that hardly fluctuates, and because its flux density of 20 Jy at 22 GHz provides a good S/N, it is recommended as a standard radio source for antenna calibration in the microwave band above 10 GHz[7][8]. The size of this radio source, moreover, is 20 arcseconds (0.005°), which means that it can be regarded as a sufficiently small point source with respect to 1.3 arcminutes (0.021°) of HPBW calculated at 22 GHz on the Kashima 34-m antenna. On the other hand, the radio source is on a galactic plane and situated in a region that involves structures, and care therefore had to be taken when pointing the reference beam. It has also been pointed out that other radio sources exist at 40 arcminutes west and 30 arcminutes southeast of the above radio source. Care in analysis was therefore required[9].

4.3 Data analysis

Figure 11 shows measured values of α based on data obtained when the main beam is not looking at the radio source in three observations of each session. Here, a tendency for $OBS\#1 \geq OBS\#2 \geq OBS\#3$ to occur in this data is thought to be due to the following. As the elevation angle decreases, the total amount of thermal noise incident on the antenna from the atmosphere increases, and in addition, thermal noise from the ground entering through side lobes makes actual $T_{Atm}(1-\exp(-\tau\sec Z))$ greater than the calculated value.

In the processing of actual observation data, the average value of α in each observation is determined from

Table 2 Meteorological data on day of observation

	Obs#1	Obs#2	Obs#3
Time (JST)	10:05	13:20	16:20
Weather	Cloudy	Cloudy/clear	Cloudy/clear
Temperature (℃)	8.9	9.1	7.9
Humidity (%)	47	47	52
Atmospheric pressure (hPa)	1022.1	1020.3	1019.9
Wind speed (m/s), wind direction	3.7 NE	3.9 ENE	1.7 ENE
τ	0.069	0.0688	0.0699
Position of radio-source DR21 in each observation			
AZ	57	65.7	314
EL	30.8	62	80.2

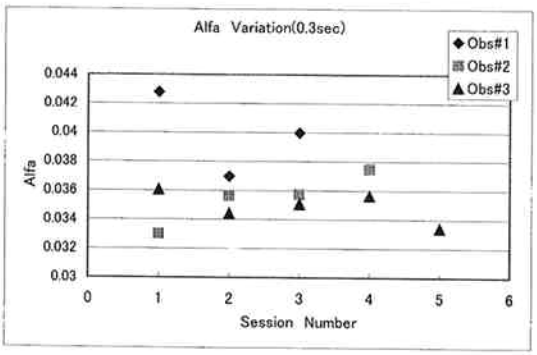

Fig. 11 Values of α for three observations in each session; value of α obtained in each observation changes

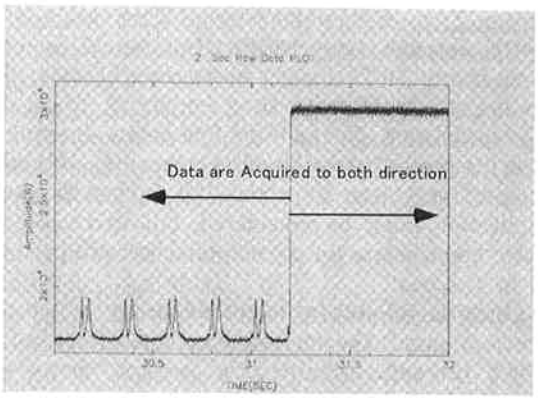

Fig. 12 Data collection method; data is collected for time periods of 0.3, 1, 3, and 20 seconds

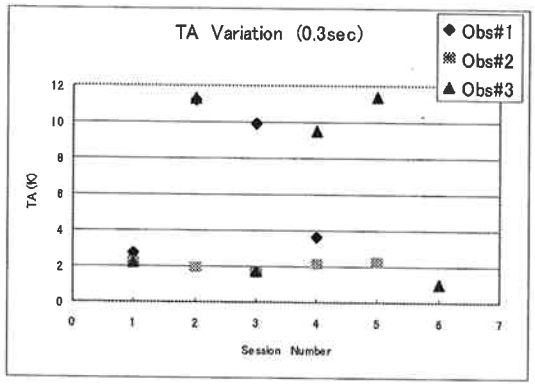

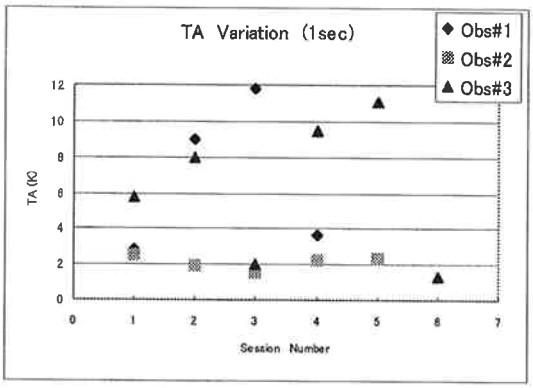

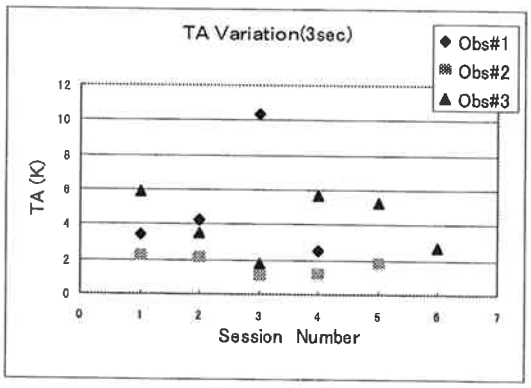

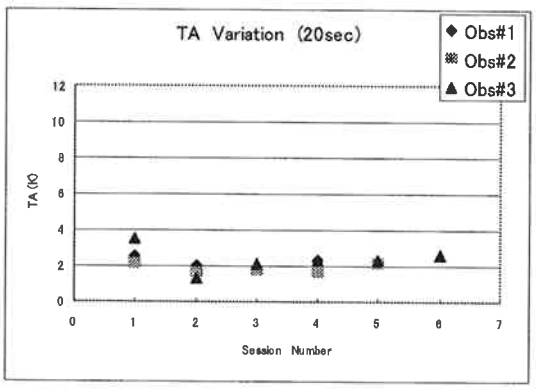

Fig. 13 T_A obtained for each data collection time period
T_A for data collection times of 0.3, 1, 3, and 20 seconds for observations in each session (when pointing the main beam at the radio source)

data obtained when the main beam is not looking at the radio source, and that average value is used in each observation as a fixed value to calculate T_A. Furthermore, in calculating T_A, we collected output data when looking at the sky immediately before switching the waveguide and output data when looking at the room-temperature radio-wave absorber immediately after, and did this for 0.3 second, 1 second, 3 seconds, and 20 seconds (Fig. 12). The values of T_A obtained in this way for each of these data collection time periods are shown in Fig. 13.

Given that flux density S_ν of the radio source is 20 Jy and assuming that the aperture efficiency of the antenna is 40%, theoretical antenna temperature T_A calculated from Eq. (5) is 2.63 K. Figure 13, however, shows that data dispersion is large for short data collection times, and data in this form cannot be expected to match up well with theoretically derived antenna temperature. On the other hand, if we extend data collection time to 20 seconds and compute T_A, we can decrease data dispersion significantly and obtain a value of 2.11K ($\pm$0.43K)

as average T_A over all observations. This result is consistent with antenna temperature that would be obtained when observing DR21 for an aperture efficiency of 40%.

Assuming an effective flux density S_ν of 20 Jy, the aperture efficiency of the Kashima 34-m antenna at 22 GHz can be computed to be 32.1% from Eqs. (6) and (7). Here, gain fluctuation (of about 1%) during 20 seconds of data collection must be considered, but this value is nevertheless appropriate in terms of observation data obtained in the past.

4.4 Evaluation of measurement accuracy

We evaluated the measurement accuracy of 2.11K (±0.43K), the value obtained for antenna temperature in this test observation. We did this by considering those parameters used in calculating antenna temperature T_A from Eq. (12) that are predicted to fluctuate, and calculated the dispersion of each over 20 seconds to evaluate the effects of each parameter on antenna temperature.

While it can be considered that error in P_{On} and P_{Off}^{Sw} should be determined independently, we note that in actuality these two values fluctuate while exhibiting the same undulation in conjunction with gain fluctuation. Evaluating the dispersion in P_{On}-P_{Off}^{Sw} is therefore a realistic approach. Table 3 lists the dispersion of each parameter and associated dispersion $(\sigma T_A)^2$ in antenna temperature.

These results tell us that the effects of P_{On}-P_{Off}^{Sw} are dominant in the dispersion $(\sigma T_A)^2$ of antenna temperature. The reason for this, it is thought, is that errors in collecting data and gain fluctuation during the 20 seconds of data collection contribute to dispersion.

The dispersion $(\sigma T_A)^2$ in antenna temperature for one session obtained from the above results is $(2.64\text{K})^2$. From this value, we get a standard deviation σT_A of 0.68K when considering the number of sessions. This agrees well with the value of 0.43K obtained from observations.

On the other hand, if we calculate minimum detection sensitivity from the effective aperture area and standard deviation of antenna temperature σT_A obtained from the above observation using Eq. (8), we get 4.1 Jy. This is a greatly inferior result compared to the ideal minimum detection sensitivity of 0.23 Jy obtained from theory[1]. This is thought to be due to the effects of random error when collecting data. In this regard, increasing the number of observations might be considered to be the most effective way of improving results, but with the current observation technique, improved sensitivity cannot be expected even if observation time is extended. There is therefore a need to investigate new techniques. At the same time, inclusion of gain fluctuation in these data results must also be considered.

As reference, we note that if we enable a room-temperature radio-wave absorber to be measured at the time of beam switching, a minimum detection sensitivity of 0.9 Jy could be forecast for 0.3-second switching over one minute based on calculations using data from this test observation. It is thought that almost no gain fluctuation is included here and that the calculated value is closer to the true value.

This test observation obtained a value of 2.11K (±0.43K) for antenna temperature T_A. This value can be considered to be somewhat appropriate, but its inclusion of gain fluctuation and large measurement error must be taken into account.

5. Summary

We have described the construction of a Dicke-type switching radiometer and the results of a test observation performed with this radiometer installed in the 22-GHz receiver of the Kashima 34-m antenna.

The value of antenna temperature T_A obtained in this observation was 2.11K (±0.43K) and the aperture efficiency of the Kashima 34-m antenna was determined from this value to be 32.1%. These values can be considered to be appropriate in terms of values predicted from calculations and on the basis of past data. Considering, however, that error is significant in data collection and that gain fluctuation is included in data, the data obtained in this test observation must be treated as reference data.

If, in the future, we enable a radio-wave absorber at room temperature to be measured at the time of beam switching, a minimum detection sensitivity of 0.9 Jy could be forecast for 0.3-second switching of one minute based on calculations using the observation data presented here. This value would exceed the minimum detection sensitivity of 2.5 Jy obtained at 15 GHz in the galactic plane survey performed by a 13.7-m telescope at Greenbank of the National Radio Astronomy Observatory (NRAO). Such a high sensitivity means that we could expect meaningful observation results in surveys and other observations performed with the Kashima 34-m antenna.

To increase sensitivity in the future, studies must be performed on upgrading the front end so as to enable a radio-wave absorber at room temperature to be measured at the time of switching. Achieving this, however, means dealing with major physical limitations, and software upgrades must also be studied to lower loss when collecting data. In addition, when increasing the quantity of obser-

Table 3 Effects of parameter error on antenna temperature T_A

Dispersion of parameters affecting antenna temperature T_A and associated dispersion $(\sigma T_A)^2$ of antenna temperature

	P_{On}- P_{Off}^{Sw}	P_{Hot}	τ	α
Parameter dispersion	115.02	117	0.000147	0.00181
$(\sigma T_A)^2$ (K)	6.67	2.95^{-3}	4.53^{-6}	0.294

vations, the difference in observation time between the main beam and reference beam means that this difference can be predicted to appear in the dispersion of data for each beam. This, together with increase in integration time, is thought to be a major cause of error in determining accuracy and must therefore be studied.

Acknowledgments

The authors would like to extend their appreciation to Tomonari Suzuyama for his patient instruction on antenna basics and for his efforts in upgrading the frequency-conversion section of the 22-GHz receiver. They would also like to thank Group Leader Tetsuro Kondo, Senior Researcher Junichi Nakajima, and everyone at the Radio Astronomy Applications Section for many helpful discussions, as well as Hiroshi Hanado and Yuko Hanado for their valuable advice on data analysis. Finally, the authors would like to express sincere thanks to on-site personnel for their yearly maintenance work on the 34-m antenna during the hot summer season.

References

(1) Kraus J. D., Radio Astronomy 2nd., Cygnus Quasar Books.

(2) Kenji Akabane, Nobuo Kaifu, Hiroto Tahara, Space Radio Astronomy, Kyoritsu Shuppan Co., Ltd.

(3) Ulich B.L., Davis J.H., Rhodes P.J., Hollis J.M., "Absolute Brightness Temperature Measurement at 3.5-mm Wavelength", IEEE Trans. Antennas Propag., vol. AP-28, No.3. May 1980.

(4) Mason B. S., Leitch E. M., Myers S.T., Cartwright J. K., Readhead A. C. S, "An Absolute Flux Density Measurement of the Supernova Remnant Cassiopeia A at 32GHz", Astron. J., 118: 2908-2918, 1999 December.

(5) M. Sekido, "System Noise Temperature", Seminar Materials, 1999/6/28.

(6) Meeks M .L., Methods of Experimental Physics Vol. 12-Part B, P-203, Academic Press.

(7) Baars J. W., Genzel R., Pauliny-Toth I.I.K., Witzel A., "The Absolute Spectrum of CasA; An Accurate Flux Density Scale and a Set of Secondary Calibrators", Astron. Astrophys., 61,99-106 (1977).

(8) Ott M., Witzel A., Quirrenbach A., Krichbaum T. P., Standke K. J., Schalinski C. J., Hummel C. A., 1994, "An updated list of radio flux density calibratiors", Astron. Astrophys., 284, 331-339.

(9) Dent W., "A Flux-Density Scale for Microwave Frequencies", Astrophys. J., 177:93-99, 1972 October 1.

(10) Langston G., Minter A., D'Addario L., Eberhardt K., Koski K., Zuber J., "The First Galactic Plane Survey at 8.35 and 14.35GHz", Astron. J., Volume 119, Issue 6, pp.2801-2827.